Physics and Chemistry of the Earth xxx (2015) xxx–xxx

Contents lists available at ScienceDirect

Physics and Chemistry of the Earth

journal homepage: www.elsevier.com/locate/pce

Temporal correlation patterns in pre-seismic electromagnetic emissions reveal distinct complexity profiles prior to major earthquakes

Reik V. Donner [a,*], Stelios M. Potirakis [b], Georgios Balasis [c], Konstantinos Eftaxias [d], Jürgen Kurths [a,e,f,g]

[a] Research Domain IV – Transdisciplinary Concepts and Methods, Potsdam Institute for Climate Impact Research, Telegrafenberg A31, 14473 Potsdam, Germany
[b] Department of Electronics Engineering, Piraeus University of Applied Sciences, 250 Thivon & P. Ralli, 12244 Aigaleo, Athens, Greece
[c] Institute for Astronomy, Astrophysics, Space Applications and Remote Sensing, National Observatory of Athens, Metaxa and Vasileos Pavlou, Penteli, 15236 Athens, Greece
[d] Section of Solid State Physics, Department of Physics, University of Athens, Panepistimiopolis, Zografos, 15784 Athens, Greece
[e] Department of Physics, Humboldt University, Newtonstraße 15, 12489 Berlin, Germany
[f] Institute for Complex Systems and Mathematical Biology, University of Aberdeen, Aberdeen AB243UE, United Kingdom
[g] Department of Control Theory, Nizhny Novgorod State University, Gagarin Avenue 23, 606950 Nizhny Novgorod, Russia

ARTICLE INFO

Article history:
Received 5 November 2014
Received in revised form 1 March 2015
Accepted 23 March 2015
Available online xxxx

Keywords:
Pre-seismic electromagnetic emissions
Earthquake preparation processes
Correlations
Dynamical complexity

ABSTRACT

In the last years, continuous recordings of electromagnetic emissions from geophysical observatories have been recognized to exhibit characteristic fluctuation patterns prior to some major earthquakes. To further evaluate and quantify these findings, this work presents a detailed assessment of the time-varying correlation properties of such emissions during the preparatory phases preceding some recent earthquakes in Greece and Italy. During certain stages before the earthquakes' occurrences, the electromagnetic variability profiles are characterized by a marked increase in the degree of organization of fluctuations, which allow developing hypotheses about the underlying physical mechanisms. Based on the preparatory phases of selected seismic events, the information provided by different statistical properties characterizing complementary aspects of the time-varying complexity based on temporal correlations is systematically assessed. The obtained results allow further insights into different pre-seismic stages based on the variability of electromagnetic emissions, which are probably associated with distinct geophysical processes.

1. Introduction

Earthquakes (EQ) are large-scale fracture phenomena arising in the Earth's heterogeneous crust, the occurrence of which is perceived in the form of a sudden violent shaking of the Earth's surface. However, the processes involved in the preparation of an EQ are complex and not easy to be directly monitored. Therefore, the view that "understanding how earthquakes occur is one of the most challenging questions in fault and earthquake mechanics" (Shimamoto and Togo, 2012) is not an overstatement. In the direction of understanding the underlying complex nonlinear processes involved in the preparation of an EQ, two research fields have attracted the particular interest of scientists. One of them, to which huge efforts have been devoted, is the study of fracture phenomena at the laboratory scale (e.g., Lockner et al., 1991; Lockner, 1996; Chauhan and Misra, 2008; Johnson et al., 2008; Baddari and Frolov, 2010; Ben-David et al., 2010; Zapperi, 2010; Baddari et al., 2011; Lacidogna et al., 2011; Hadjicontis et al., 2011; Schiavi et al., 2011; Carpinteri et al., 2012; Chang et al., 2012), while the other is the study of different phenomena which are observed in the field prior to the occurrence of significant EQs.

It has been shown that opening cracks are accompanied with electro-magnetic emissions (EME) covering a wide frequency spectrum from the kHz band to the MHz band. These signals can be found at the laboratory scale prior to global failure in fracture experiments (e.g., Chauhan and Misra, 2008; Baddari et al., 2011; Lacidogna et al., 2011; Hadjicontis et al., 2011; Carpinteri et al., 2012), as well as at the geophysical scale prior to significant EQs (e.g., Warwick et al., 1982; Hayakawa and Fujinawa, 1994; Qian et al., 1994; Gokhberg et al., 1995; Kapiris et al., 2004; Contoyiannis et al., 2005, 2015; Uyeda et al., 2009; Cicerone et al., 2009; Potirakis et al., 2012, 2013, 2015; Eftaxias et al., 2013; Eftaxias and Potirakis, 2013). Two important features of EME have been observed in both the laboratory and the field: (i) emissions in the MHz band consistently precede those in the kHz band, indicating that each type of those emissions corresponds to different characteristic stages of the fracture/EQ preparation, while

* Corresponding author. Tel.: +49 331 288 2064; fax: +49 331 288 2640.
E-mail addresses: reik.donner@pik-potsdam.de (R.V. Donner), spoti@teipir.gr (S. M. Potirakis), gbalasis@noa.gr (G. Balasis), ceftax@phys.uoa.gr (K. Eftaxias), juergen.kurths@pik-potsdam.de (J. Kurths).

http://dx.doi.org/10.1016/j.pce.2015.03.008
1474-7065/

(ii) after the emission of the kHz EME an electro-magnetic quiescence systematically emerges before the time of the global failure/EQ occurrence (Kumar and Misra, 2007; Qian et al., 1994; Baddari and Frolov, 2010; Hayakawa and Fujinawa, 1994; Gokhberg et al., 1995; Matsumoto et al., 1998; Hayakawa, 1999; Eftaxias et al., 2013; Eftaxias and Potirakis, 2013; and references therein). Based on these features and the results obtained through the analysis of field observations of MHz-kHz EME by multidisciplinary time-series analysis tools, the following four-stage model of the EQ preparation process by means of fracture-induced EME has been proposed recently (Eftaxias and Potirakis, 2013, and references therein; Contoyiannis et al., 2015, and references therein):

(1) The initially emerging MHz EM field is attributed to cracking in the highly disordered material that surrounds the backbone of strong entities (asperities) distributed around the stressed fault sustaining the system. It has been shown using the Method of Critical Fluctuations (MCF) that this emission shows anti-persistency and can be described in analogy to a thermal second-order phase transition in equilibrium (Contoyiannis et al., 2005, and references therein). More detailed analysis by means of truncated Lévy statistics and non-extensive Tsallis statistical mechanics suggests that a truncated Lévy walk-type mechanism can organize the heterogeneous system to criticality (Contoyiannis and Eftaxias, 2008). Importantly, based on the recently introduced method of natural time analysis (Varotsos et al., 2011a, b), it has been shown that the seismic activity that occurs in the region around the epicenter of the forthcoming significant shock a few days up to approximately one week before the main shock occurrence, as well as the observed MHz EM precursor which emerges during the same period of time, both behave as critical phenomena (Potirakis et al., 2013, 2015).
(2) Our understanding of different rupture modes is still very much in its infancy. However, laboratory experiments of rock fracture and frictional sliding have shown that the relative slip of two fault surfaces takes place in two phases: a slow stick–slip like fracture-sliding precedes dynamical fast global slip (Ben-David et al., 2010; Chang et al., 2012). It has been suggested that the abrupt emergence of a strong avalanche-like kHz EM field is due to the fracture of the family of the asperities themselves, namely to the slow stick–slip like stage of the rupture mode. This emission exhibits a high information content and organization, a preferred direction in the underlying fracto-EM mechanism and persistency, i.e., it includes key features of an extreme event (Eftaxias et al., 2013; Eftaxias and Potirakis, 2013; and references therein). The observed kHz EM precursor is characterized by the absence of any footprint of a second-order transition in equilibrium or a truncated Lévy walk-type mechanism. On the contrary, it shows footprints of a first-order phase transition (Contoyiannis et al., 2015). The kHz EM time series includes well-established universal structural patterns of fracture-faulting processes, namely: (i) the activation of a single fault by means of kHz EM activity behaves as a reduced/magnified image of the regional/laboratory seismicity; (ii) its temporal profile is consistent with the universal fractional Brownian motion-type spatial profile of natural rock surfaces; (iii) the roughness of its temporal profile coincides with the universal spatial roughness of fracture surfaces. Finally, the kHz EM emission is consistent with the fault modeling of the occurred earthquake, which is supported by studies from different disciplines, e.g., satellite radar interferometry and seismology (Eftaxias et al., 2013; Eftaxias and Potirakis, 2013; and references therein).
(3) Recently, it has been shown by means of the MCF that in between the above mentioned two stages of the fracture process, there exists an intermediate stage which reflects the tri-critical behavior (Contoyiannis et al., 2015). This stage appears in the kHz EME just before the emergence of the strong avalanche-like kHz emission. The results obtained for the kHz time series are compatible with those for an introduced model map which describes the tri-critical crossover. The tri-critical crossover indicates the boundary of an anti-persistent dynamics, namely the existence of a negative feedback mechanism that kicks the system away from extreme behavior.
(4) The systematically observed EM quiescence in all frequency bands is rooted in the stage of preparation of dynamical slip, which results in the fast, even super-shear, mode that surpasses the shear wave speed. Recent laboratory experiments also reveal this feature.

In summary, the proposed four stages of the last part of EQ preparation process and the associated EM observables appear in the following order: 1st stage: valid MHz anomaly; 2nd stage: kHz anomaly exhibiting tri-critical characteristics; 3rd stage: strong avalanche-like kHz anomaly; 4th stage: electromagnetic quiescence.

We note that the study of EME possibly related with an upcoming significant seismic event is associated with the existence of "*paradox features*" that accompany their observation, expressed in the form of the following research questions: Why is EM quiescence observed at the time of the EQ occurrence? Why are the emerging EM signals not accompanied by large precursory strain changes, much larger than co-seismic ones? Why are the EM emissions not observed during the aftershock period? How is the traceability of potential EM precursors achieved given that they should normally be absorbed by the Earth's crust? A first attempt to answering these questions has been recently presented (Eftaxias et al., 2013; Eftaxias and Potirakis, 2013; and references therein).

The above suggested four-stage model of EQ preparation processes by means of fracture-induced EME is a hypothesis that remains to be further verified. However, it should be noted that, up to now, it seems to be in agreement with both experimental (laboratory and geophysical) data, as well as theoretic and simulation studies of fracture phenomena, while no rebuttal has been published yet.

In this work, we focus on the third stage and the analysis of the strong avalanche-like kHz EME; all the herein analyzed signals are strong avalanche-like kHz anomalies, corresponding to the same stage, the third stage, of our proposed four-stage model. Due to the important practical implications of the hypothesis that these emissions signify the fracture of asperities, which means that after the observation of valid recorded kHz signals the EQ occurrence is inevitable, it is crucial to apply further analysis methods which help identifying those features embedded in the kHz EME that could possibly reveal the validity of such recordings. As it was mentioned, a crucial footprint of an extreme event is its high degree of organization. Such a feature should be included in a fracto-EM activity rooted in the fracture of asperities. It is important to note that "there is no way to find an optimum organization or complexity measure" (Kurths et al., 1995). Therefore, in this work we search for further evidence for the (temporary) existence of a dynamical state of high organization, which clearly discriminates an emerging kHz anomaly prior to a large EQ from the background EM noise in the region of the recording station. For this purpose, we utilize different measures characterizing the dynamical complexity of geophysical signals based on their linear correlation structure, an approach that has been originally proposed by Donner and Witt (2006, 2007) in a multivariate framework and

Please cite this article in press as: Donner, R.V., et al. Temporal correlation patterns in pre-seismic electromagnetic emissions reveal distinct complexity profiles prior to major earthquakes. J. Phys. Chem. Earth (2015), http://dx.doi.org/10.1016/j.pce.2015.03.008

recently been adopted for defining an easily calculable complexity measure for univariate time series (Donner and Balasis, 2013). In this work, we complement the previously developed analysis strategy by a suite of additional measures quantifying different aspects associated with the correlation structure of pre-seismic EME.

The remainder of this manuscript is organized as follows: Section 2 describes the EME data used in this study. The analysis methodology used in this work is detailed in Section 3. Subsequently, the results of our investigations are presented in Section 4 and put into the context of previous findings in Section 5.

2. Data

The kHz EME time series analyzed in the present work have all been recorded at the exemplary remote telemetric station at Zakynthos (Zante) Island in the Ionian Sea (western Greece), using instrumentation developed by Nomicos (Nomikos et al., 1997). Zakynthos Island is located at a region of high tectonic activity, right on the Hellenic Arc (Kopanas, 1997), cf. Fig. 1. The telemetric station has been installed on a carefully selected mountainous site at the south-west of the island (37.76° N, 20.76° E) providing at the same time very low background noise and high Earth conductivity (Antonopoulos, 1996; Makris et al., 1999; Eftaxias et al., 2001). These features render this specific station particularly appropriate for magnetic field strength measurements, i.e. for kHz EME detection. The kHz EME are measured by six loop antennas detecting the three components, east–west (EW), north–south (NS), and vertical, of the variations of the magnetic field at 3 kHz and 10 kHz, respectively. The EME time series are sampled once per second, i.e., with a sampling frequency of 1 Hz. More information about the experimental setup can be found in the supplementary material of Potirakis et al. (2015).

The analyzed kHz EME time series were detected prior to three significant EQs which happened in Greece and Italy, cf. Fig. 1. In chronological order, these EQs are the Kozani-Grevena EQ [occurred on 13 May 1995 (08:47:13 UT) in northern Greece with an epicenter at 40.17° N, 21.68° E and a magnitude of 6.5] (e.g., Kapiris et al., 2002, 2003; Eftaxias et al., 2002; Contoyiannis et al., 2005), the Athens EQ [with magnitude 5.9, occurred on 7 September 1999 (11:56:49 UT) in central Greece (38.15° N, 23.62° E)] (e.g., Eftaxias et al., 2004, 2007; Kapiris et al., 2004; Contoyiannis et al., 2005; Karamanos et al., 2005, 2006; Kalimeri et al., 2008), and the L'Aquila EQ [with magnitude 6.3, occurred on 06 April 2009 (01:32:41 UT) in central Italy (42.34° N, 13.38° E)] (e.g., Eftaxias, 2009; Eftaxias et al., 2009, 2010). More specifically, the following data have been analyzed for these three cases: (i) different kHz EM variations (10 kHz NS and EW, 3 kHz NS, EW and vertical) recorded during a 3 days period from 11 May 1995, 00:00:00 (UT), to 13 May 1995, 23:59:59 (UT), for the Kozani-Grevena EQ, (ii) 10 kHz NS EM variations recorded during an 11 days period from 28 August 1999, 00:00:00 (UT) to 7 September 1999, 23:59:59 (UT), for the Athens EQ, and (iii) 10 kHz EW EM variations recorded during a 3 days period from 3 April 2009, 00:00:00 (UT), to 5 April 2009, 23:59:59 (UT), for the L' Aquila EQ. The corresponding time series are shown in Figs. 2 and 3.

We clarify that the above mentioned observed potential EM precursors are associated with very shallow EQs that occurred on land with magnitude ~6 or larger. The associated fracture processes are extended up to the surface of the Earth. Thus the produced fracto-electromagnetic emission can be directly launched to the atmosphere (Eftaxias and Potirakis, 2013 and references therein). In turn, comparable signatures of deeper EQs are commonly harder to observe.

3. Methods

In this work, we utilize several novel approaches for characterizing dynamical complexity of geophysical signals based on their linear correlation structure.

In a univariate setting, the quantification of serial correlations has been traditionally restricted to relatively simple statistical properties like the de-correlation time (i.e., the time lag after which correlations have decayed below a certain level), the lag-one auto-correlation coefficient (or, equivalently, the coefficient of a first-order auto-regressive (AR(1)) process fitted to the data for describing correlated noise as some kind of statistical null-model to geophysical time series, cf., e.g., Torrence and Compo (1999)), or the Hurst exponent H related to the power-law exponent of the auto-correlation function (ACF) for large lags in the

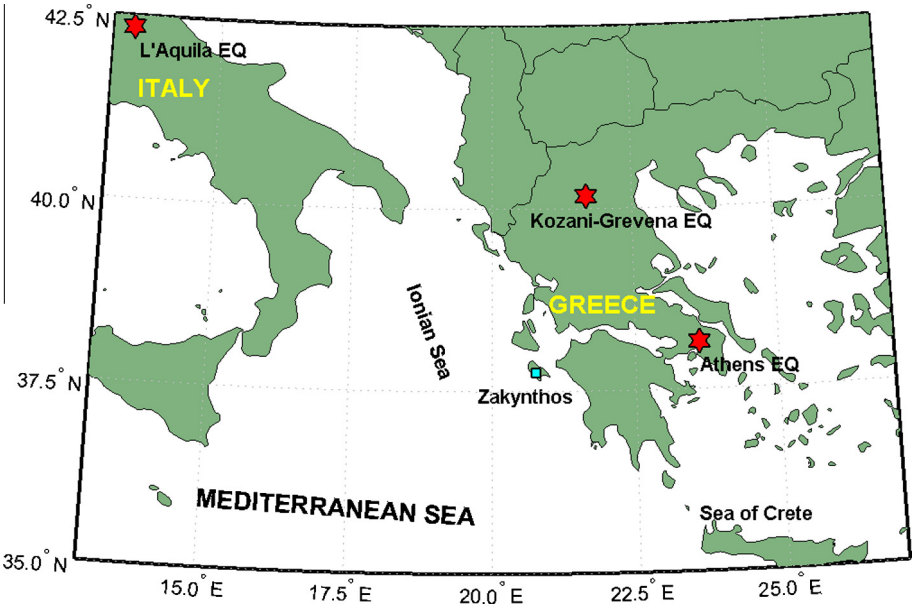

Fig. 1. Location of the recording station at Zakynthos as well as the epicenters of the three studied EQs.

Please cite this article in press as: Donner, R.V., et al. Temporal correlation patterns in pre-seismic electromagnetic emissions reveal distinct complexity profiles prior to major earthquakes. J. Phys. Chem. Earth (2015), http://dx.doi.org/10.1016/j.pce.2015.03.008

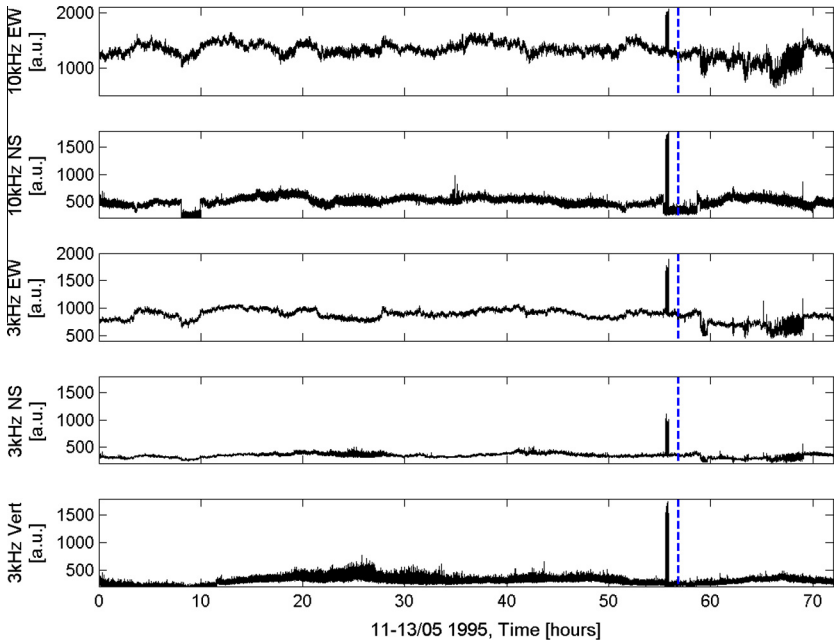

Fig. 2. Studied pre-seismic kHz EME time series associated with the Kozani-Grevena EQ (five components). The dashed blue line indicates the timing of the mainshock. (For interpretation of the references to color in this figure legend, the reader is referred to the web version of this article.)

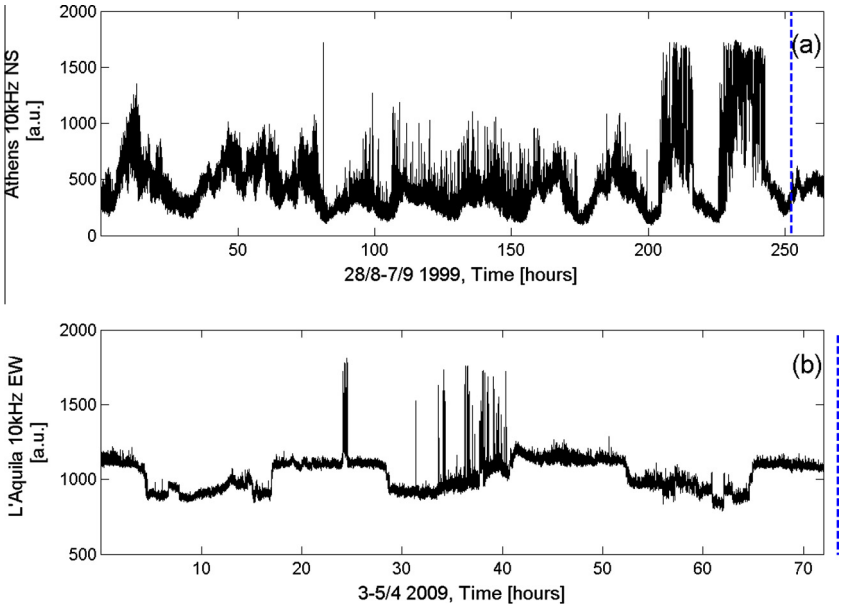

Fig. 3. The analyzed pre-seismic kHz EME around the Athens (a) and L'Aquila (b) EQs. The dashed blue lines indicate the timing of the corresponding mainshocks. (For interpretation of the references to color in this figure legend, the reader is referred to the web version of this article.)

presence of long-term memory. Notably, the latter parameter is commonly estimated using alternative approaches like the power spectral density, wavelets or detrended fluctuation analysis (Peng et al., 1994) due to their better stability properties in comparison with estimating H directly from the ACF. In the field of pre-seismic EME, the Hurst exponent has already been used to characterize the persistent/anti-persistent properties of the signal, as well as to reveal that the universal spatial roughness of fracture surfaces ($H \sim 0.7$) nicely coincides with the roughness of the temporal profile of the recorded kHz EM precursors (Ponson et al., 2006; Mourot et al., 2006; Lopez and Schmittbuhl, 1998; Zapperi et al., 2005; Hansen and Schmittbuhl, 2003; Renard et al., 2006; Potirakis et al., 2011).

Here, we follow a distinctively different approach by viewing the correlation structure of geophysical time series from a multivariate perspective. For this purpose, we consider the cross-correlation matrix $\boldsymbol{C}$ of the lagged trajectory matrix consisting of m replications of the original time series mutually shifted by a fixed time step τ (equivalently, we can unfold the ACF coefficients at lags $\tau, 2\tau, \ldots, (m-1)\tau$ into a symmetric Toeplitz matrix having constant entries on all diagonals). The corresponding approach is widely applied in terms of singular spectrum analysis (SSA, cf. Broomhead and King, 1986; Ghil et al., 2002) used for a variety of applications such as spectral analysis or gap filling in geophysical data. Instead of further following this methodology, we aim at globally characterizing the statistical properties associated with

Please cite this article in press as: Donner, R.V., et al. Temporal correlation patterns in pre-seismic electromagnetic emissions reveal distinct complexity profiles prior to major earthquakes. J. Phys. Chem. Earth (2015), http://dx.doi.org/10.1016/j.pce.2015.03.008

this (positive semi-definite) correlation matrix. For this purpose, we study the associated spectrum of non-negative real eigenvalues of $\boldsymbol{C}$. Specifically, we utilize different characteristics inspired by findings for correlation matrices in various other fields like financial markets (Plerou et al., 2002), neurophysiology (Müller et al., 2005) and spatio-temporal chaos (Zoldi and Greenside, 1997).

First, we study the largest eigenvalue σ_1^2, which can be interpreted as the fraction of variance of the m-dimensional embedded system explained by its first principal component. The participation ratio of the associated eigenvector $(a_{11},\ldots,a_{1m})$ (Plerou et al., 2002; Müller et al., 2005)

$$\pi_1 = \left(m \sum_{j=1}^{m} |a_{1j}|^4 \right)^{-1} \tag{1}$$

characterizes how strong different lags contribute to this component. Due to the fourth power of the eigenvector coefficients, directions in the embedding space (i.e., time lags) contributing strongly to the first eigenvector receive much stronger weight than those having minor relevance. Hence, if there are only a few relevant time lags, the sum will be large, so that π_1 takes small values. In turn, in case of a more balanced distribution (i.e., more time lags contributing significantly to the first principal component, pointing to a more complex signal), we may expect higher values of π_1.

Second, we compute the normalized Shannon entropy of the full spectrum of eigenvalues $\sigma_1^2,\ldots,\sigma_m{}^2$ of $\boldsymbol{C}$ as follows: The eigenvalues are first normalized to unit sum. Then, we take the decadal logarithms of the normalized eigenvalues. The relative frequencies p_k of logarithmic normalized eigenvalues to fall into K bins ($k = 1,\ldots,K$) of the same size are evaluated and used for estimating the associated normalized Shannon entropy

$$S = \frac{1}{\log K} \sum_{k=1}^{K} p_k \log p_k. \tag{2}$$

High values of S indicate a broad variety of eigenvalues (i.e., few dominating "modes"), whereas smaller values correspond to situations where the eigenvalue spectrum is more concentrated (i.e., there are many different "variability patterns" associated with different combinations of time lags, which have comparable relevance). Note that in order to assure quantitative comparability of the results for different data sets and/or time slices, the same binning needs to be considered. The number of bins K is to be selected such that each bin contains on average a statistically sufficient number of eigenvalues, i.e., needs to be properly chosen according to the value of m. To our best knowledge, the Shannon entropy of the eigenvalue spectrum of $\boldsymbol{C}$ has not yet been used elsewhere for the purpose of characterizing the time-varying degree of dynamical complexity of geophysical or other time series and thus presents a novel methodological aspect of the present work. We emphasize that the eigenvalue entropy S is not to be confused with the classical Shannon entropy of the underlying signal itself, since it quantifies distinctively different properties of the data under study. Specifically, when evaluated in terms of block or permutation entropies, high values of the Shannon entropy commonly indicate higher dynamical disorder pointing to possibly higher complexity of the underlying signal. In turn, high values of the eigenvalue entropy indicate a broad range of eigenvalues, i.e., variability modes contained in the correlation structure of the data tend to have different variances instead of similar ones, which could be interpreted as a signature of low complexity.

Finally, we study the scaling of residual SSA variances when more and more eigenvalues of $\boldsymbol{C}$ are considered. For this purpose, consider again the eigenvalues $\sigma_i{}^2$ normalized to unit sum. The difference between 1 and the sum of the first p normalized eigenvalues gives the residual fraction of variance not explained by the first p principal components of $\boldsymbol{C}$ (in SSA language, the first p reconstructed components). It has been found numerically that in many cases, the residual variances show a roughly exponential decay. The typical scale parameter associated with this decay is called the linear variance decay (LVD) dimension density (Donner and Witt, 2006, 2007; Donner et al., 2008). This parameter is estimated by means of linear regression up to a given maximum fraction of explained variance $f = 0.9$ (see Donner et al. (2008) for full details on the estimation procedure). Considering the limiting cases of fully uncorrelated and perfectly linearly correlated components, a normalized LVD dimension density δ can be defined, which takes values of $\delta = 0$ for perfect correlations (i.e., a deterministic signal with constant values or some linear trend) and $\delta = 1$ for vanishing serial correlations (i.e., white noise), respectively (Xie et al., 2011). While the original approach has been developed for multivariate time series, its modification for univariate records has recently found several applications (Toonen et al., 2012; Donner and Balasis, 2013).

We emphasize that the four statistical parameters σ_1^2, π_1, S and δ characterize different aspects associated with the correlation structure of the signal under study. Specifically, the latter two can be interpreted as measures of disorder and complexity of the correlation structure. Motivated by recent proposals for combining conceptually similar pairs of measures in some complexity-entropy plane (Martin et al., 2006; Rosso et al., 2007), we will mainly focus on δ and S in order to distinguish time intervals with different dynamical regimes in the pre-seismic kHz EME.

4. Results

4.1. Auto-correlation functions

Since all measures used in this study are based on the traditional Pearson correlation, it appears justified to start our analysis by inspecting the structure of the ACFs associated with the different kHz pre-seismic EME records. Notably, the behavior of the ACF can reveal important information on typical time-scales of fluctuations contained in the signal. For our corresponding analysis, we first take the global picture by disregarding the possible distinction into different phases prior and even after the occurrence of the mainshock.

From Fig. 4, we conclude that all considered records show marked non-stationarity expressed in terms of a generally very slow decay of the ACFs for all considered signals. This effect is to be expected given the different levels of kHz EME amplitudes during different stages of the EQ preparation processes as well as its immediate aftermath (cf. Figs. 2 and 3), which dominate the ACF when evaluated at this global scale. In order to address the problem of non-stationarity at the level of mean EME amplitudes (but not the superimposed short-term fluctuations), all records were subjected to a moving-average detrending regarding mean values taken over centered windows in time with a width of 30 min. After this pre-processing, the data actually exhibit a relatively fast decay of serial correlations as expected for approximately stationary time series.

Looking in somewhat more detail at the shape of the ACFs, we find that the recordings for the L'Aquila and Athens EQs display a smooth decay without any pronounced oscillatory components. The corresponding behavior is distinctively different for the Kozani-Grevena EQ, where the five different recorded kHz EME components exhibit somewhat different correlation patterns. Specifically, in three of the five components (10 kHz EW, 3 kHz EW and 3 kHz NS) the ACF appears modulated with a signal of about 265 s period, while the two other components (10 kHz NS and 3 kHz vertical) exhibit similar but much faster modulations

Please cite this article in press as: Donner, R.V., et al. Temporal correlation patterns in pre-seismic electromagnetic emissions reveal distinct complexity profiles prior to major earthquakes. J. Phys. Chem. Earth (2015), http://dx.doi.org/10.1016/j.pce.2015.03.008

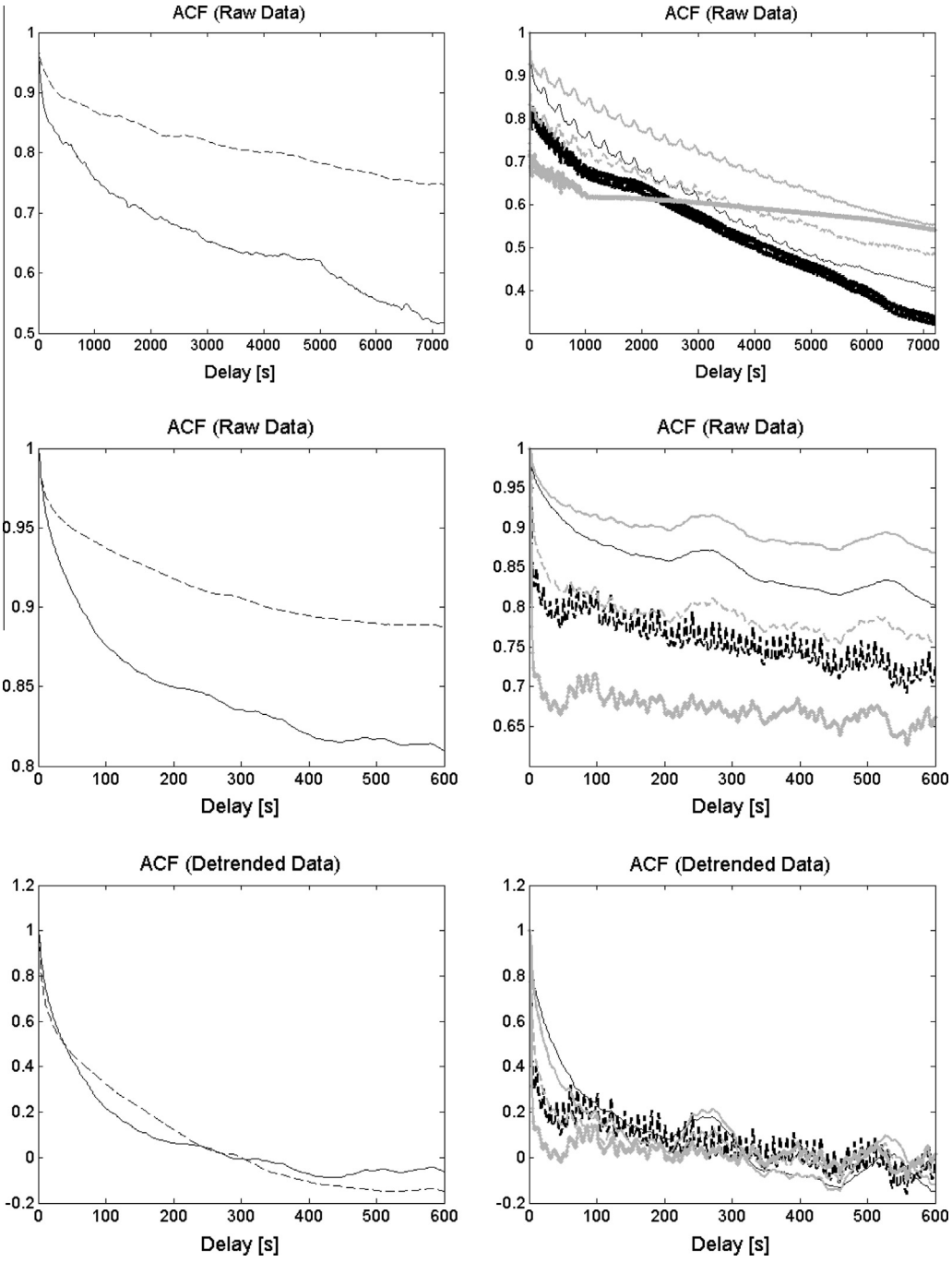

Fig. 4. Auto-correlation functions (ACFs) for the short excerpts of the kHz pre-seismic EME data described in Section 2. From top to bottom: ACFs for time-scales up to 3 h for the raw data, zooms thereof for time-scales up to 10 min, and short-term ACF for data after removing running means taken over 30 min of data. Left panels: data from the L'Aquila (solid) and Athens (dashed) EQs. Right panels: all available components from the Kozani-Grevena EQ (10 kHz: black, 3 kHz: grey, EW: solid, NS: dashed, vertical: dash-dotted).

with periods of about 10 s. However, spectral analysis (not shown) reveals that there are no significant oscillatory components embedded in the observed signal, so that we rather have to relate them to sampling effects. In addition, we observe that for the 3 kHz vertical component, the behavior of the raw data ACF changes markedly at time-scales of about 1000 s from highly variable correlation values at shorter time lags to a much smoother behavior at longer scales.

Due to these complex features of the data, in what follows all analyses of short-term fluctuations have been performed in parallel on the raw and the running-mean detrended data. Since we are examining the short-term fluctuations of the EME for running windows in time of at most 1 h size, it can be noted that the previously discussed non-stationarity of the records commonly does not dominate the correlation structure on these time scales, so that the obtained results are almost independent of whether raw or detrended data have been used (not shown).

4.2. Temporal correlation patterns I: L'Aquila EQ

We start our detailed investigation of time-dependent dynamical complexity with the relatively short EME record associated with the L'Aquila EQ. Fig. 5 illustrates that the auto-correlation structure of the time series is far from being constant over time.

Please cite this article in press as: Donner, R.V., et al. Temporal correlation patterns in pre-seismic electromagnetic emissions reveal distinct complexity profiles prior to major earthquakes. J. Phys. Chem. Earth (2015), http://dx.doi.org/10.1016/j.pce.2015.03.008

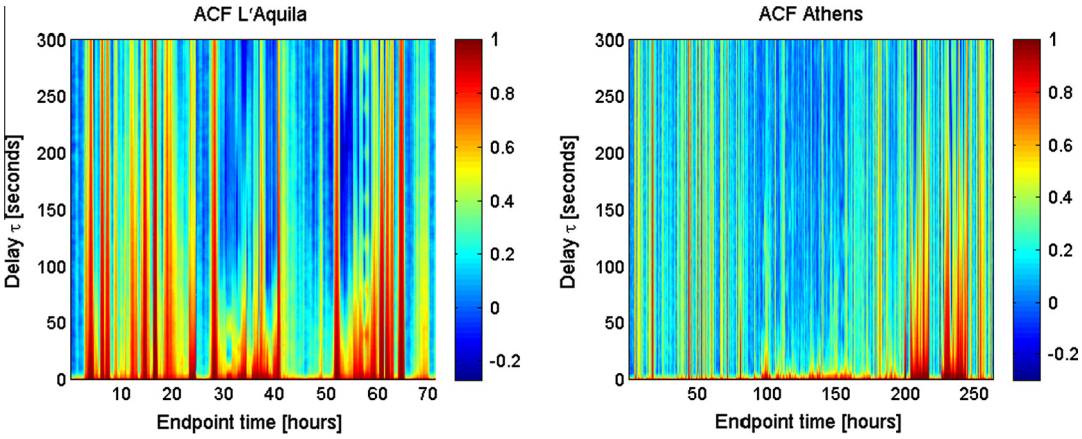

Fig. 5. Time-dependent ACF (color-coded) up to a maximum lag of 5 min for running windows of 1 h and mutual offset of 1 min for the kHz EME record associated with the L'Aquila and Athens EQs. (For interpretation of the references to color in this figure legend, the reader is referred to the web version of this article.)

In contrast, we observe alternations between sequences of time windows with very fastly and very slowly decaying ACF, suggesting qualitatively different physical processes causing the corresponding emissions. Notably, a slow decay of correlations is a common manifestation of long-range dependences, whereas a fast decay can often be observed in case of anti-persistent dynamics. We do not address the aspect of persistence here, since it is relatively hard to evaluate in the relatively short time windows used here for a characterization of time-varying dynamical complexity. A more detailed corresponding study will be subject of future work.

Based the observed complex temporal variability of autocorrelations, we proceed with calculating the different characteristics introduced in Section 3. The results of this investigation are shown in Figs. 6 and 7 for a window width of 1 h and mutual offset of 1 min. Regarding the AR(1) coefficient, the largest eigenvalue σ_1^2 and its associated participation ratio π_1 (Fig. 6), the observed variability appears mutually consistent and mainly traces the aforementioned succession of time intervals with fast and slow ACF decay, respectively. In turn, the eigenvalue entropy S and LVD dimension density δ (Fig. 7) exhibit a more interesting pattern prior to the EQ, although the complexity measure mainly co-varies with the AR(1) coefficient and the information associated with the leading eigenvalue. The latter behavior is to be expected, however, we emphasize that differences in the temporal profile of δ from that of the other characteristics indicate a more complex distribution of eigenvalues, deviating significantly from the presumed exponential decay of residual variances underlying this measure.

Examining Fig. 7 in more detail, we find that there are time intervals during which δ drops to values close to 0, some of which are in parallel characterized by a marked increase of S. The latter periods can be found between about 23 and 41 h after the beginning of the record, while the EQ itself occurred at around 73.5 h and was unfortunately not covered by the available EME record. Intermittent to the aforementioned time interval, there are periods with lower (but still gradually increasing) eigenvalue entropy and higher (gradually decreasing) complexity. This intermittent behavior is obviously associated with pronounced spikes in the EME signal, cf. Fig. 3b. Finally, the time interval between 41 h after the start of measurements and the EQ occurrence is characterized by (apart from an intermediate time window between about 52 and 60 h) high values of δ, while S fluctuates around its relatively low baseline level. Notably, in contrast to δ, S does not exhibit any further

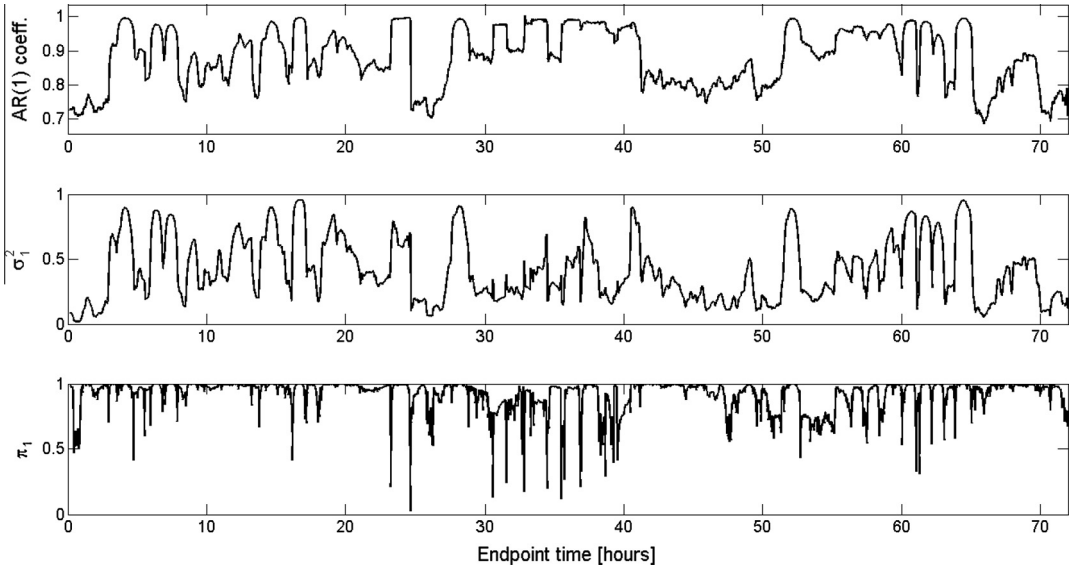

Fig. 6. Correlation-based characteristics for the L'Aquila EQ (computed for running windows of width 1 h, mutual offset of 1 min): AR(1) coefficient, largest eigenvalue σ_1^2 and associated participation ratio π_1.

Please cite this article in press as: Donner, R.V., et al. Temporal correlation patterns in pre-seismic electromagnetic emissions reveal distinct complexity profiles prior to major earthquakes. J. Phys. Chem. Earth (2015), http://dx.doi.org/10.1016/j.pce.2015.03.008

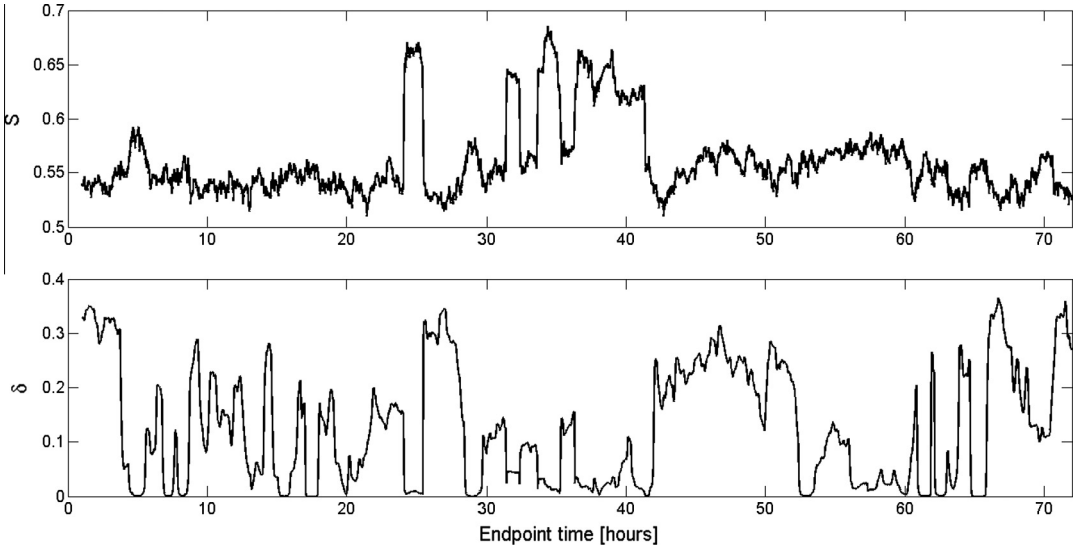

Fig. 7. Eigenvalue entropy S and LVD dimension density δ for the L'Aquila EQ (same windows as in Fig. 6).

marked maxima, whereas the LVD dimension density exhibits short periods of low complexity until about 7–8 h prior to the L'Aquila EQ.

In summary, the most striking features of our analysis of the L'Aquila EQ-related emissions are (i) a time interval of about 50–32 h prior to the mainshock, which is characterized by intermittent high entropy (high dynamical disorder) and low complexity following gradual trends and (ii) a period of high dynamical complexity and low eigenvalue entropy directly prior to the EQ. The first observation could be a manifestation of the fracture of pre-existing fragments filling the gap between the rough profiles of the fault, while the second is consistent with the fracture of the strong entities (asperities) sustaining the system (Minadakis et al., 2012). The fact that there are no further indications of periods with high eigenvalue entropy in the remaining part of the considered record suggests its possible relationship with the final dynamical process related to the EQ preparation, i.e., the stage of preparation of the dynamical slip which results in the fast, even super-shear, mode that surpasses the shear wave speed after the end of the slow stick–slip like stage of rupture mode related to the fracture of asperities (Eftaxias et al., 2013; Eftaxias and Potirakis, 2013; and references therein).

However, the considered record alone is too short to draw justified conclusions about the possible significance of the previously reported findings as potential EQ precursors. Therefore, it will be of interest if similar observations can be made for the two other considered EQs as well.

4.3. Temporal correlation patterns II: Athens EQ

We performed the same analysis as before for the 11-days EME recordings prior to and shortly after the Athens EQ. In general, the observations regarding the temporal variability of the ACF are qualitatively similar to those for the L'Aquila EQ (though exhibiting a different "microscopic" pattern, cf. Fig. 5), so that we directly focus on the eigenvalue entropy S and LVD dimension density δ in the following.

The corresponding results are shown in Fig. 8. It can be noted that very similar to the L'Aquila EQ, we again observe an opposite trend of eigenvalue entropy (upward) and our complexity measure

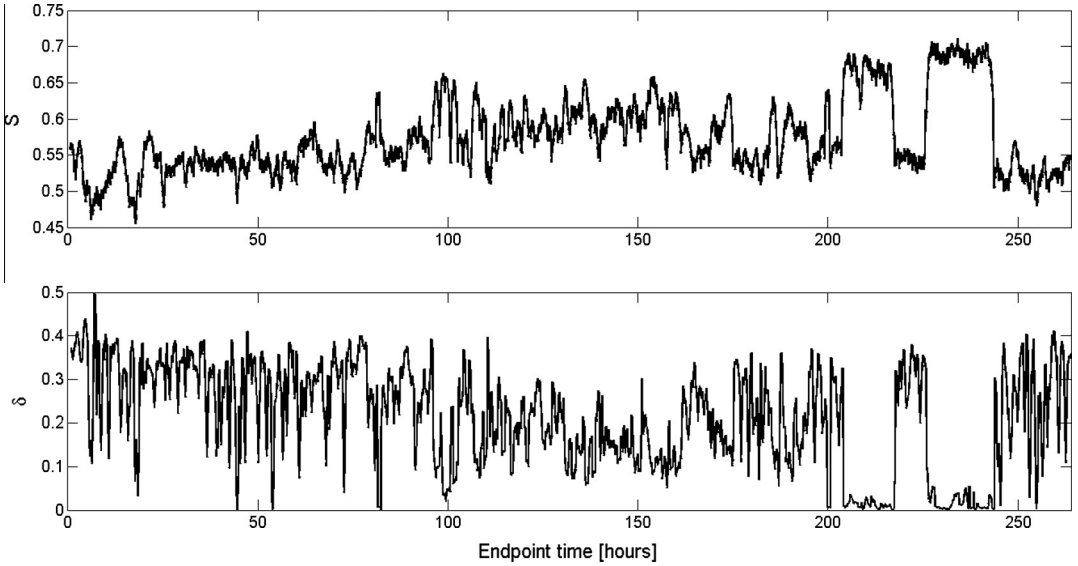

Fig. 8. As in Fig. 7 for the Athens EQ.

Please cite this article in press as: Donner, R.V., et al. Temporal correlation patterns in pre-seismic electromagnetic emissions reveal distinct complexity profiles prior to major earthquakes. J. Phys. Chem. Earth (2015), http://dx.doi.org/10.1016/j.pce.2015.03.008

(downward) during some extended time period before the main shock (about 0–160 h after the beginning of the considered record, the EQ occurred at about 255 h). Moreover, the time interval immediately prior to the EQ is again characterized by two extended time intervals with high entropy and low complexity followed by conditions with low entropy and high complexity. Unlike for the L'Aquila EQ, this alternating behavior can be directly observed in the amplitude of EME (cf. Fig. 3a). In the Athens case, we find a low-complexity and high-entropy state of kHz EME between about 205 and 215 h and about 225 and 245 h after the beginning of the record. In turn, between about 215 and 225 h as well as immediately before the EQ occurrence, we have also a period of high dynamical complexity and low entropy as in the L'Aquila EQ case, which is attributed to EM quiescence. It is also worth mentioning that an intermittent state with short (and faster) alternating periods of (low–high) complexity and (high-low) entropy can be identified from about 87 h to about 205 h indicating a different underlying mechanism responsible for these kHz EME. Finally, there is a gradual trend of increasing entropy/decreasing complexity as approaching the mainshock, which abruptly stops a few hours before the EQ occurrence (after the two extended time intervals with high entropy and low complexity).

We conclude that the observed temporal complexity profile is qualitatively similar to that of the L'Aquila EQ, although the relevant processes prior to the Athens EQ appear to develop on considerably longer time scales than in the previous case. Specifically, our analysis seems to clearly reveal three different phases: (i) a phase with strongly fluctuating complexity and entropy levels (~87 h to ~205 h), (ii) two similar low dynamical complexity phases of longer duration (~205 h to ~245 h) interrupted by a time interval of high complexity (~215 h to ~225 h), (iii) a phase of high dynamical complexity during the last ~10 h before the EQ occurrence.

4.4. Temporal correlation patterns III: Kozani-Grevena EQ

After the previous encouraging results for the L'Aquila and Athens EQs, we now take a deeper look at the recordings prior to the Kozani-Grevena EQ. From the overall correlation structure of the five measured kHz EME components (Fig. 4), it can be expected that the corresponding behavior is more complex than for the two other EQs and significantly differs among the different components. This is confirmed by the results of our analysis presented in Fig. 9.

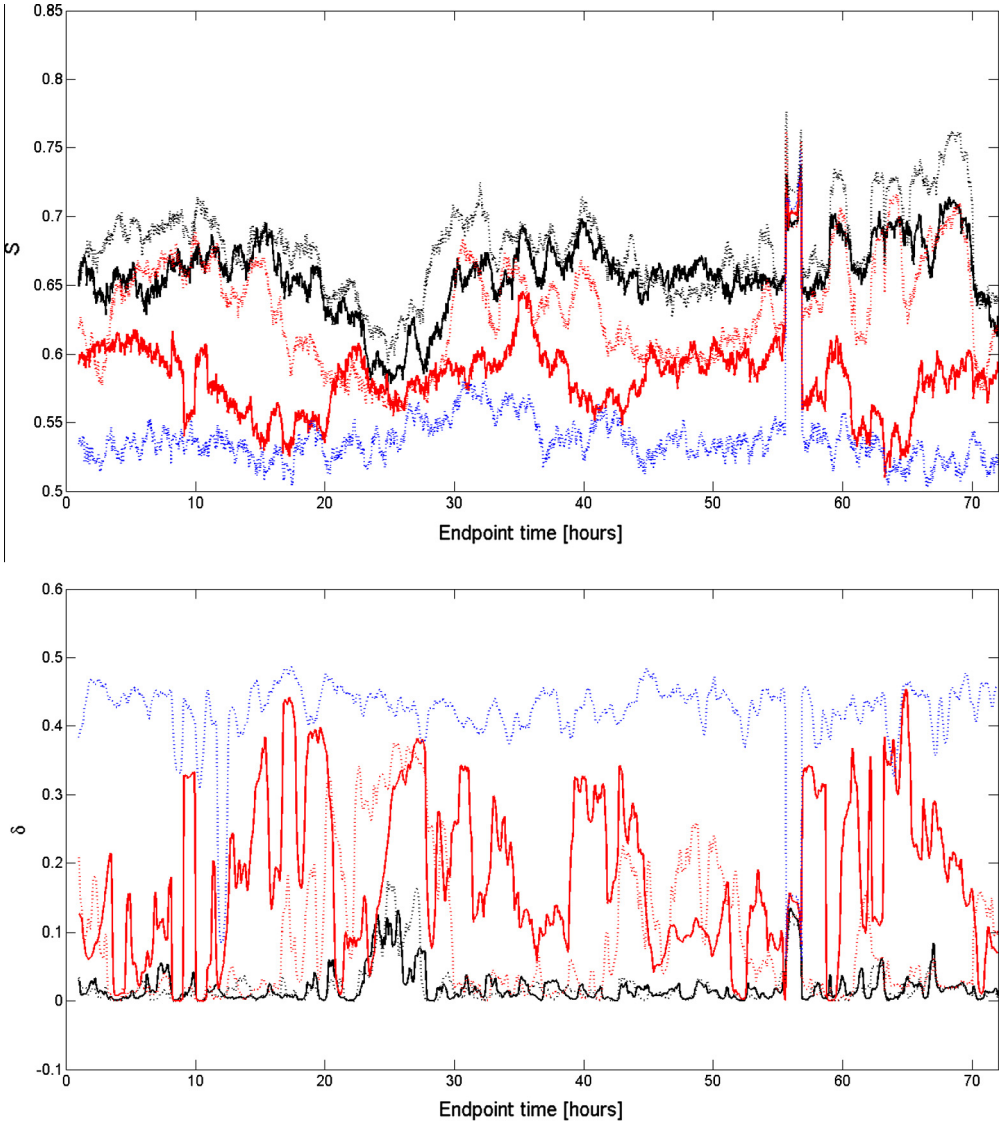

Fig. 9. As in Fig. 7 for the Kozani-Grevena EQ. Different colors and line styles indicate the different recorded EME components: 10 kHz (solid) vs. 3 kHz (dotted), EW (black), NS (red) and vertical (blue). (For interpretation of the references to color in this figure legend, the reader is referred to the web version of this article.)

Please cite this article in press as: Donner, R.V., et al. Temporal correlation patterns in pre-seismic electromagnetic emissions reveal distinct complexity profiles prior to major earthquakes. J. Phys. Chem. Earth (2015), http://dx.doi.org/10.1016/j.pce.2015.03.008

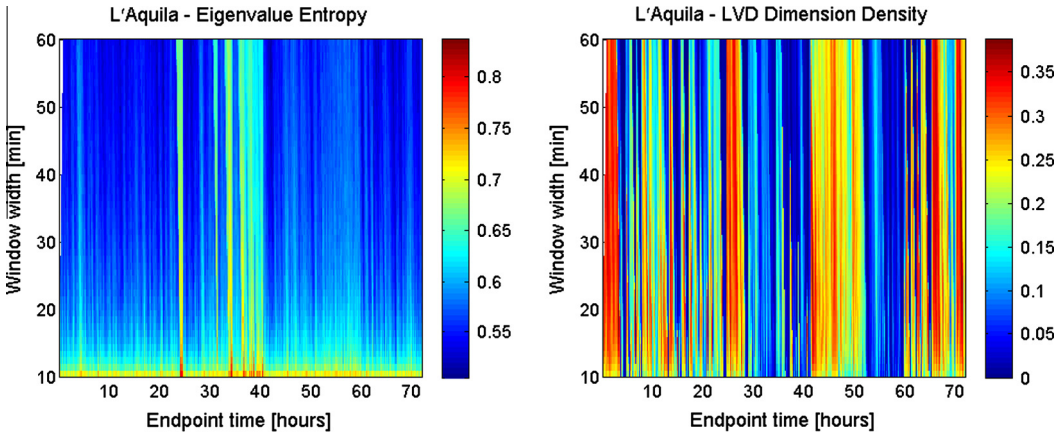

Fig. 10. Dependence of the temporal variation of the eigenvalue entropy S and the LVD dimension density δ (color-coded) on the considered window size w for the L'Aquila case. (For interpretation of the references to color in this figure legend, the reader is referred to the web version of this article.)

First of all, we note that the 3 kHz vertical component (dotted blue line in Fig. 9) exhibits a constantly lower eigenvalue entropy and higher LVD dimension density than the other four components. Taken together, and considering the rather atypical behavior of the ACF for this component (Fig. 4), we conclude that it most likely exhibits more stochastic variability than actually interpretable pre-seismic EM signal. Therefore, we will disregard it in the following. In a similar way, we do not further interpret the results for the 10 kHz NS component (solid red line in Fig. 9), since the overall variability of the two considered measures is distinctively different from the three remaining components, which is again in agreement with the different global ACF properties. A notable exception is the short time period around 55–56 h after the beginning of the record, which is characterized by a short peak in all five EME components relatively shortly (∼1 h) before the EQ and shows up in both eigenvalue entropy and LVD dimension density. Notably, this short period appears to be the only distinct time interval of high dynamical disorder observed so far in the analysis of the Kozani-Grevena EQ-related kHz EM that could be associated with the current model of EQ preparation processes detailed in Section 1. As far the two measures studied in this work are concerned, we observe different tendencies in the abrupt change of δ apparently depending on the associated baseline levels in the different components. In turn, we observe a consistent local peak in the eigenvalue entropies associated with all five components, followed by lower entropy values that extend up to the occurrence of the mainshock and shortly (about 1 h) after. This observation is in agreement with the general picture obtained from the analysis of the time series associated with the other two EQs.

Besides this short time period of increased eigenvalue entropy, the most interesting non-trivial complexity feature of the three components 10 kHz EW, 3 kHz EW and 3 kHz NS arises between about 15 and 30 h after the beginning of the record and displays a gradual decrease followed by another increase back to the previous level for the eigenvalue entropy, and the opposite behavior for the LVD dimension density. In comparison with the sharp transitions between opposite behaviors found prior to the two other EQs, this feature is clearly less pronounced, and its possible relationship to some distinct EQ preparation processes remains ambiguous. However, the general tendency appears similar as for the two other EQs and could just be masked in the Kozani-Grevena EQ-related record due to some event-specific conditions (e.g., related to the respective geological setting in terms of heterogeneity of the geological structure around the fault, pre-existing fragmentation, etc.).

4.5. Robustness of the results

The results reported above have been consistently obtained for a given window size of one hour. In order to examine their robustness if this parameter is changed, we have performed a corresponding systematic investigation by varying the window widths between 10 min and one hour. Given that we are looking for time-dependent signatures associated with dynamical complexity encoded in the ACF structure, we prefer not to consider larger windows here, while 10 min was chosen as a lower bound to guarantee a sufficiently large statistical sample for the calculation of the ACF within each window up to a maximum delay of 5 min. The corresponding results are exemplarily shown in Fig. 10 for the case of the L'Aquila EQ and demonstrate the high degree of consistency between the variability observed for different window widths. Notably, for smaller windows the samples considered for evaluating the ACF also become smaller, which results – together with the higher intrinsic variation – in a higher variability of the different window-wise measures, keeping the previously discussed overall picture unchanged.

Further robustness checks could be undertaken regarding the maximum delay in the ACF, the step in the delay, as well as (in case of the LVD dimension density) the maximum fraction of explained variance considered in the estimation. For the conciseness of this contribution, we do not report the corresponding results here, but emphasize that for moderate variations of these parameters, no significant changes of our results are to be expected.

5. Conclusions

The presented analysis has revealed some common features among the kHz EME time series recorded prior to three recent significant EQs in Greece and Italy. First of all, there is a common opposite trend of complexity (decreasing) and the newly introduced measure eigenvalue entropy (increasing) as approaching the time of occurrence of the mainshock. Moreover, in all three cases, relatively long entropy peaks emerge a few hours before the EQ, while immediately following them low eigenvalue entropy conditions are observed up to the time of occurrence of the EQ.

In the kHz EME recorded prior to the L'Aquila and Athens EQs, one can clearly distinguish a systematically complementary behavior of the employed complexity metrics (eigenvalue entropy and LVD dimension density), implying three phases probably related to different underlying mechanisms associated with the preparation of an EQ:

Please cite this article in press as: Donner, R.V., et al. Temporal correlation patterns in pre-seismic electromagnetic emissions reveal distinct complexity profiles prior to major earthquakes. J. Phys. Chem. Earth (2015), http://dx.doi.org/10.1016/j.pce.2015.03.008

(i) A first characteristic phase of intermittent fluctuations in the eigenvalue entropy dominates a time interval of a few tens of hours prior to the mainshock. This phase is characterized by a relatively low initial baseline level of eigenvalue entropy and a high initial baseline level of dynamical complexity, which exhibit gradual trends towards higher entropy and lower complexity.
(ii) A second phase is characterized by extended periods of low dynamical complexity and high eigenvalue entropy, which can be interrupted by time intervals of opposite characteristics. This second phase is terminated shortly (a few hours) prior to the EQ. As suggested by our findings for the L'Aquila EQ, the first two phases may at least partially overlap.
(iii) The final phase is characterized by a state of low eigenvalue entropy and high complexity following right after the second phase, persisting up to the time of occurrence of the EQ and possibly beyond.

The first phase could be a manifestation of the fracture of pre-existing fragments filling the gap between the rough profiles of the fault, while the second appears consistent with the signatures to be expected for a fracture of the strong entities (asperities) sustaining the system. The last phase signalizes the preparation of the dynamical slip, which results in the fast, even super-shear, mode that surpasses the shear wave speed and is perceived as the main EQ event. The first two phases fall into the third stage of the four-stage model of the EQ preparation process by means of fracture-induced EME mentioned in Section 1, providing a finer partitioning of this stage consistent with other already published results (Minadakis et al., 2012). In turn, the third phase would be consistent with the fourth stage of the aforementioned model.

In terms of the employed complexity metrics, the kHz EME recorded prior to the Kozani-Grevena EQ behave differently from those prior to the L'Aquila and Athens EQs, not clearly presenting all the above features. This finding could be due to the different shape of the corresponding spectra as a result of different data quality, as suggested by the presented analysis, or to different dynamics related to the different geological structure around the corresponding focal volumes. It is noted that the power spectrum of the Kozani-Grevena kHz activity reveals two different power-laws, one for the low frequencies and another for the high frequencies [Fig. 4 in Kapiris et al. (2004)]. The high frequency power-law may reflect the dynamics within the bursts of the kHz emissions while the low frequency one may indicate the correlation between the bursts. It should also be noted that the lead-time and the duration of the detected kHz EM anomaly before the Kozani-Grevena EQ were much shorter than in the other two cases, especially compared to the Athens kHz EME. These differences are probably a result of the fact that the Kozani-Grevena focal area has a more homogeneous geological structure, while it is less fragmented, since the Kozani-Grevena is a region of low historical seismic activity (Contoyiannis et al., 2015).

We emphasize that the presented analysis provides first indications for a refinement of the mechanistic model of EQ preparation processes through temporal correlation patterns in pre-seismic electromagnetic emissions and the associated distinct complexity profiles. Due to the limited amount of data considered here for the pre-mainshock period, we cannot yet draw any final conclusions about whether or not the herein revealed complexity and eigenvalue entropy signatures are truly unique to the preparatory stages of major EQs. However, to this end we do not have any results supporting the occurrence of similar patterns outside the EQ preparation process. A corresponding analysis will be subject of future work. In addition, we underline the necessity of a further in-depth characterization of the three identified phases by means of complementary statistical as well as nonlinear dynamics tools, such as breakpoint regression for the observed trends in complexity and eigenvalue entropy or a deeper investigation of the scaling characteristics of the kHz EME during the different phases and the relevant time-scales involved in them by means of, e.g., wavelet analysis. We are confident that such future analyses can help further constraining the physical mechanisms underlying the reported temporal complexity profiles and may thus provide another important step towards a better understanding of EQ preparation processes.

Conflict of interest

The authors declare no conflict of interest.

Acknowledgements

This work has been financially supported by the joint Greek-German project "Transdisciplinary assessment of dynamical complexity in magnetosphere and climate: A unified description of the nonlinear dynamics across extreme events" funded by IKY and DAAD. RVD acknowledges additional support by the German Federal Ministry for Education and Research via the BMBF Young Investigator's Group CoSy-CC^2 (Grant no. 01LN1306A). Technical assistance by M. Wiedermann in performing the presented numerical analyses was very much appreciated. GB acknowledges additional support from the European Union Seventh Framework Programme (FP7-REGPOT-2012-2013-1) under grant agreement no. 316210 (BEYOND – Building Capacity for a Centre of Excellence for EO-based monitoring of Natural Disasters).

References

Antonopoulos, G., 1996. Modeling the geoelectric structure of Zante Island from MT measurements. Ph. D. thesis, University of Athens (in Greek).
Baddari, K., Frolov, A., 2010. Regularities in discrete hierarchy seismo-acoustic mode in a geophysical field. Ann. Geophys. 53, 31–42.
Baddari, K., Frolov, A., Tourtchine, V., Rahmoune, F., 2011. An integrated study of the dynamics of electromagnetic and acoustic regimes during failure of complex macrosystems using rock blocks. Rock Mech. Rock Eng. 44, 269–280.
Ben-David, O., Cohen, G., Fineberg, J., 2010. The dynamic of the onset of frictional slip. Science 330, 211–214.
Broomhead, D.S., King, G.P., 1986. Extracting qualitative dynamics from experimental data. Physica D 20, 217–236.
Carpinteri, A., Lacidogna, G., Manuello, A., Niccolini, G., Schiavi, A., Agosto, A., 2012. Mechanical and electromagnetic emissions related to stress-induced cracks. SEM Exp. Techniq. 36, 53–64.
Chang, J., Lockner, D., Reches, Z., 2012. Rapid acceleration leads to rapid weakening in earthquake-like laboratory experiments. Science 338, 101–105.
Chauhan, V., Misra, A., 2008. Effects of strain rate and elevated temperature of electromagnetic radiation emission during plastic deformation and crack propagation in ASTM B 265 grade 2 Titanium sheets. J. Math. Sci. 43, 5634–5643.
Cicerone, R.D., Ebel, J.E., Britton, J., 2009. A systematic compilation of earthquake precursors. Tectonophysics 476, 371–396.
Contoyiannis, Y., Eftaxias, K., 2008. Tsallis and Levy statistics in the preparation of an earthquake. Nonlin. Proc. Geophys. 15, 379–388.
Contoyiannis, Y.F., Kapiris, P.G., Eftaxias, K.A., 2005. A Monitoring of a pre-seismic phase from its electromagnetic precursors. Phys. Rev. E 71, 066123.
Contoyiannis, Y., Potirakis, S.M., Eftaxias, K., Contoyianni, L., 2015. Tricritical crossover in earthquake preparation by analyzing preseismic electromagnetic emissions. J. Geodyn. 84, 40–54.
Donner, R.V., Balasis, G., 2013. Correlation-based characterisation of time-varying dynamical complexity in the Earth's magnetosphere. Nonlin. Proc. Geophys. 20, 965–975.
Donner, R., Witt, A., 2006. Characterisation of long-term climate change by dimension estimates of multivariate palaeoclimatic proxy data. Nonlin. Proc. Geophys. 13, 485–497.
Donner, R., Witt, A., 2007. Temporary dimensions of multivariate data from paleoclimate records – a novel measure for dynamic characterization of long-term climate change. Int. J. Bifurcation Chaos 17, 3685–3689.
Donner, R., Sakamoto, T., Tanizuka, N., 2008. Complexity of spatio-temporal correlations in Japanese air temperature records. In: Donner, R.V., Barbosa, S.M. (Eds.), Nonlinear Time Series Analysis in the Geosciences – Applications in Climatology, Geodynamics, and Solar-Terrestrial Physics. Springer, Berlin, pp. 125–154.

Eftaxias, K., 2009. Footprints of nonextensive Tsallis statistics, selfaffinity and universality in the preparation of the L'Aquila earthquake hidden in a pre-seismic EM emission. Physica A 389, 133–140.
Eftaxias, K., Potirakis, S.M., 2013. Current challenges for pre-earthquake electromagnetic emissions: shedding light from micro-scale plastic flow, granular packings, phase transitions and self-affinity notion of fracture process. Nonlin. Proc. Geophys. 20, 771–792.
Eftaxias, K., Kapiris, P., Polygiannakis, J., Bogris, N., Kopanas, J., Antonopoulos, G., Peratzakis, A., Hadjicontis, V., 2001. Signature of pending earthquake from electromagnetic anomalies. Geophys. Res. Lett. 28, 3321–3324.
Eftaxias, K., Kapiris, P., Dologlou, E., Kopanas, J., Bogris, N., Antonopoulos, G., Peratzakis, A., Hadjicontis, 2002. EM anomalies before the Kozani earthquake: a study of their behavior through laboratory experiments. Geophys. Res. Lett. 29, 1228.
Eftaxias, K., Frangos, P., Kapiris, P., Polygiannakis, J., Kopanas, J., Peratzakis, A., Skountzos, P., Jaggard, D., 2004. Review-model of pre-seismic electromagnetic emissions in terms of fractal-electrodynamics. Fractals 12, 243–273.
Eftaxias, K., Panin, V.E., Ye, Deryugin Ye., 2007. Evolution-EM signals before earthquakes in terms of meso-mechanics and complexity. Tectonophysics 431, 273–300.
Eftaxias, K., Athanasopoulou, L., Balasis, G., Kalimeri, M., Nikolopoulos, S., Contoyiannis, Y., Kopanas, J., Antonopoulos, G., Nomicos, C., 2009. Unfolding the procedure of characterizing recorded ultra low frequency, kHZ and MHz electromagnetic anomalies prior to the L'Aquila earthquake as pre-seismic ones – Part 1. Nat. Hazards Earth Syst. Sci. 9, 1953–1971.
Eftaxias, K., Balasis, G., Contoyiannis, Y., Papadimitriou, C., Kalimeri, M., Athanasopoulou, L., Nikolopoulos, S., Kopanas, J., Antonopoulos, G., Nomicos, C., 2010. Unfolding the procedure of characterizing recorded ultra low frequency, kHZ and MHz electromagnetic anomalies prior to the L'Aquila earthquake as pre-seismic ones – Part 2. Nat. Hazards Earth Syst. Sci. 10, 275–294.
Eftaxias, K., Potirakis, S.M., Chelidze, T., 2013. On the puzzling feature of the silence of precursory electromagnetic emissions. Nat. Hazards Earth Syst. Sci. 13, 2381–2397.
Ghil, M., Allen, R.M., Dettinger, M.D., Ide, K., Kondrashov, D., Mann, M.E., Robertson, A.W., Saunders, A., Tian, Y., Varadi, F., Yiou, P., 2002. Advanced spectral methods for climatic time series. Rev. Geophys. 40, 3.
Gokhberg, M.K., Morgounov, V.A., Pokhotelov, O.A., 1995. Earthquake Prediction: Seismo-Electromagnetic Phenomena. Gordon and Breach, Singapore.
Hadjicontis, V., Mavromatou, C., Mastrogiannis, D., Antsygina, T.N., Chishko, K.A., 2011. Relationship between electromagnetic and acoustic emissions during plastic deformation of gamma-irradiated LiF monocrystals. J. Appl. Phys. 110, 024907.
Hansen, A., Schmittbuhl, J., 2003. Origin of the universal roughness exponent of brittle fracture surfaces:stress-weighted percolation in the damage zone. Phys. Rev. Lett. 90, 45504–45507.
Hayakawa, M., 1999. Atmospheric and Ionospheric Electromagnetic Phenomena Associated with Earthquakes. Terrapub, Tokyo.
Hayakawa, M., Fujinawa, Y., 1994. Electromagnetic Phenomena Related to Earthquake Prediction. Terrapub, Tokyo.
Johnson, P., Savage, H., Knuth, M., Gomberg, J., Marone, C., 2008. Effects of acoustic waves on stick-slip in granular media and implications for earthquakes. Nature 451, 57–60.
Kalimeri, M., Papadimitriou, K., Balasis, G., Eftaxias, K., 2008. Dynamical complexity detection in pre-seismic emissions using nonadditive Tsallis entropy. Physica A 387, 1161–1172.
Kapiris, P., Polygiannakis, J., Peratzakis, A., Nomikos, K., Eftaxias, K., 2002. VHF-electromagnetic evidence of the underlying pre-seismic critical stage. Earth Planets Space 54, 1237–1246.
Kapiris, P., Eftaxias, K., Nomikos, K., Polygiannakis, J., Dologlou, E., Balasis, G., Bogris, N., Peratzakis, A., Hadjicontis, V., 2003. Evolving towards a critical point: a possible electromagnetic way in which the critical regime is reached as the rupture approaches. Nonlin. Proc. Geophys. 10, 511–524.
Kapiris, P., Eftaxias, K., Chelidze, T., 2004. Electromagnetic signature of prefracture criticality in heterogeneous media. Phys. Rev. Lett. 92, 065702.
Karamanos, K., Peratzakis, A., Kapiris, P., Nikolopoulos, S., Kopanas, J., Eftaxias, K., 2005. Extracting pre-seismic electromagnetic signatures in terms of symbolic dynamics. Nonlin. Proc. Geophys. 12, 835–848.
Karamanos, K., Dakopoulos, D., Aloupis, K., Peratzakis, A., Athanasopoulou, L., Nikolopoulos, S., Kapiris, P., Eftaxias, K., 2006. Pre-seismic electromagnetic signals in terms of complexity. Phys. Rev. E 74, 016104.
Kopanas, J., 1997. Precursory seismoelectromagnetic anomalies recorded by Zakynthos station. Ph. D. thesis, University of Athens (in Greek).
Kumar, R., Misra, A., 2007. Some basic aspects of electromagnetic radiation emission during plastic deformation and crack propagation in Cu-Zn alloys. Mater. Sci. Eng. A 454, 203–210.
Kurths, J., Voss, A., Saparin, P., Witt, A., Kleiner, H., Wessel, N., 1995. Quantitative analysis of heart rate variability. Chaos 5, 88–94.
Lacidogna, G., Carpinteri, A., Manuello, A., Durin, G., Schiavi, A., Niccolini, G., Agosto, A., 2011. Acoustic and electromagnetic emissions as precursors phenomena in failure processes. Strain 47 (Suppl. 2), 144–152.
Lockner, D., 1996. Brittle fracture as an analog to earthquakes: can acoustic emission be used to develop a viable prediction strategy? J. Acoustic Emission 14, 88–101.
Lockner, D., Byerlee, J., Kuksenko, V., Ponomarev, A., Sidorin, A., 1991. Quasi-static fault growth and shear fracture energy in granite. Nature 350, 39–42.
Lopez, J., Schmittbuhl, J., 1998. Anomalous scaling of fracture surfaces. Phys. Rev. E 57, 6405–6408.
Makris, J., Bogris, N., Eftaxias, K., 1999. A new approach in the determination of characteristic directions of the geoelectric structure using Mohr circles. Earth Planets Space 51, 1059–1065.
Martin, M.T., Plastino, A., Rosso, O.A., 2006. Generalized statistical complexity measures: geometrical and analytical properties. Physica A 369, 439–462.
Matsumoto, H., Ikeya, M., Yamanaka, C., 1998. Analysis of barberpole color and speckle noises recorded 6 and half hours before the Kobe earthquake. Jpn. J. App. Phys. 37, 1409–1411.
Minadakis, G., Potirakis, S.M., Nomicos, C., Eftaxias, K., 2012. Linking electromagnetic precursors with earthquake dynamics: an approach based on nonextensive fragment and self-affine asperity models. Physica A 391, 2232–2244.
Mourot, G., Morel, S., Bouchaud, E., Valentin, G., 2006. Scaling properties of mortar fracture surfaces. Int. J. Fract. 140, 39–54.
Müller, M., Baier, G., Galka, A., Stephani, U., Muhle, H., 2005. Detection and characterization of changes of the correlation structure in multivariate time series. Phys. Rev. E 71, 046116.
Nomikos, K., Vallianatos, F., Kaliakatsos, I., Sideris, E., Bakatsakis, M., 1997. The latest aspects of telluric and electromagnetic variations associated with shallow and intermediate depth earthquakes in the South Aegean. Ann. Geofis. 40, 361–374.
Peng, C.-K., Buldyrev, S.V., Havlin, S., Simons, M., Stanley, H.E., Goldberger, A.L., 1994. Mosaic organization of DNA nucleotides. Phys. Rev. E 49, 1685–1689.
Plerou, V., Gopikrishnan, P., Rosenow, B., Amaral, L.A.N., Guhr, T., Stanley, H.E., 2002. Random matrix approach to cross correlations in financial data. Phys. Rev. E 65, 066126.
Ponson, L., Bonamy, D., Bouchaud, E., 2006. Two-dimensional scaling properties of experimental fracture surfaces. Phys. Rev. Lett. 96, 035506.
Potirakis, S.M., Minadakis, G., Nomicos, C., Eftaxias, K., 2011. A multidisciplinary analysis for traces of the last state of earthquake generation in preseismic electromagnetic emissions. Nat. Hazards Earth Syst. Sci. 11, 2859–2879.
Potirakis, S.M., Minadakis, G., Eftaxias, K., 2012. Relation between seismicity and pre-earthquake electromagnetic emissions in terms of energy, information and entropy content. Nat. Hazards Earth Syst. Sci. 12, 1179–1183.
Potirakis, S.M., Karadimitrakis, A., Eftaxias, K., 2013. Natural time analysis of critical phenomena: the case of pre-fracture electromagnetic emissions. Chaos 23, 023117.
Potirakis, S.M., Contoyiannis, Y., Eftaxias, K., Koulouras, G., Nomicos, C., 2015. Recent field observations indicating an Earth system in critical condition before the occurrence of a significant earthquake. IEEE Geosc. Remote Sens. Lett. 12, 631–635.
Qian, S., Yian, J., Cao, H., Shi, S., Lu, Z., Li, J., Ren, K., 1994. Results of the observations on seismo-electromagnetic waves at two earthquake areas in China. In: Hayakawa, M., Fujinawa, Y. (Eds.), Electromagnetic Phenomena Related to Earthquake Prediction. Terrapub, Tokyo, pp. 205–211.
Renard, F., Voisin, C., Marsan, D., Schmittbuhl, J., 2006. High resolution 3D laser scanner measurements of a strike-slip fault quantity its morphological anisotropy at all scales. Geophys. Res. Lett. 33, L04305.
Rosso, O.A., Larrondo, H.A., Martin, M.T., Plastino, A., Fuentes, M.A., 2007. Distinguishing noise from chaos. Phys. Rev. Lett. 99, 154102.
Schiavi, A., Niccolini, G., Terrizzo, P., Carpinteri, A., Lacidogna, G., Manuello, A., 2011. Acoustic emissions at high and low frequencies during compression tests in brittle materials. Strain 47, 105–110.
Shimamoto, T., Togo, T., 2012. Earthquakes in the Lab. Science 338, 54–55.
Toonen, C., Lappe, D., Donner, R., Scholz-Reiter, B., 2012. Impact of machine-driven capacity constellations on performance and dynamics of job-shop systems. In: ElMaraghy, H.A. (Ed.), Enabling Manufacturing Competetiveness and Economic Sustainability. Springer, Berlin, pp. 611–616.
Torrence, C., Compo, G.P., 1999. A practical guide to wavelet analysis. Bull. Amer. Meteorol. Soc. 79, 61–78.
Uyeda, S., Nagao, T., Kamogawa, M., 2009. Short-term earthquake prediction: current status of seismo-electromagnetics. Tectonophysics 470, 205–213.
Varotsos, P.A., Sarlis, N.V., Skordas, E.S., 2011a. Natural Time Analysis: The New View of Time. Springer, Heidelberg.
Varotsos, P., Sarlis, N.V., Skordas, E.S., Uyeda, S., Kamogawa, M., 2011b. Natural time analysis of critical phenomena. Proc. Natl. Acad. Sci. U.S.A. 108, 11361–11364.
Warwick, J.W., Stoker, C., Meyer, T.R., 1982. Radio emission associated with rock fracture: Possible application to the great Chilean earthquake of May 22 1960. J. Geophys. Res. 87 (B4), 2851–2859.
Xie, X., Zhao, X., Fang, Y., Cao, Z., He, G., 2011. Normalized linear variance decay dimension density and its application of dynamical complexity detection in physiological (fMRI) time series. Phys. Lett. A 375, 1789–1795.
Zapperi, S., 2010. Looking at how things slip. Science 330, 184–185.
Zapperi, S., Kumar, P., Nukala, V., Simunovic, S., 2005. Crack roughness and avalanche precursors in the random fuse model. Phys. Rev. E 71, 026106.
Zoldi, S.M., Greenside, H.M., 1997. Karhunen-Loéve decomposition of extensive chaos. Phys. Rev. Lett. 78, 1687–1690.

Please cite this article in press as: Donner, R.V., et al. Temporal correlation patterns in pre-seismic electromagnetic emissions reveal distinct complexity profiles prior to major earthquakes. J. Phys. Chem. Earth (2015), http://dx.doi.org/10.1016/j.pce.2015.03.008